74.

PAGEOPH, Vol. 134, No. 3 (1990)

0033-4553/90/030333-22$1.50 + 0.20/0

M_m: A Variable-period Mantle Magnitude for Intermediate and Deep Earthquakes

EMILE A. OKAL[1]

Abstract—We extend to the case of intermediate and deep earthquakes the mantle magnitude developed for shallow shocks by OKAL and TALANDIER (1989). Specifically, from the measurement of the spectral amplitude of Rayleigh waves at a single station, we obtain a mantle magnitude, M_m, theoretically related to the seismic moment of the event through

$$M_m = \log_{10} M_0 - 20.$$

The computation of M_m involves two corrections. The distance correction is the same as for shallow shocks. For the purpose of computing the frequency-dependent source correction, we define three depth windows: Intermediate (A) (75 to 200 km); Intermediate (B) (200–400 km) and Deep (over 400 km). In each window, the source correction C_S is modeled by a cubic spline of $\log_{10} T$.

Analysis of a dataset of 200 measurements (mostly from GEOSCOPE stations) shows that the seismic moment of the earthquakes is recovered with a standard deviation of 0.23 units of magnitude, and a mean bias of only 0.14 unit. These figures are basically similar to those for shallow events. Our method successfully recognizes truly large deep events, such as the 1970 Colombia shock, and errors due to the potential misclassification of events into the wrong depth window are minimal.

Key words: Mantle magnitude, Rayleigh waves, deep sources.

1. *Introduction and Background*

The purpose of this paper is to extend to intermediate and deep earthquakes the mantle magnitude M_m introduced for shallow events by OKAL and TALANDIER (1989). In that paper (hereafter "Paper I"), we were motivated principally, for the purpose of accurate tsunami warning, by the need to obtain a reliable, one-station estimate of the seismic moment M_0 of a teleseismic event, if at all possible in real time (i.e., while seismic waves are still being recorded). One of the most important results of Paper I was that, because of its variable-period character, our approach successfully eliminated the saturation effects, rendering the use of the classical "Richter" magnitude M_s inadequate (and even possibly dangerous for tsunami prevention), when M_0 grows beyond a few times 10^{27} dyn-cm. We further showed

---

[1] Department of Geological Sciences, Northwestern University, Evanston, Illinois 60208, U.S.A.

(TALANDIER and OKAL, 1989) that our procedure could be automated, and implemented on a simple Personal Computer.

Following traditional seismological nomenclature, we define intermediate and deep earthquakes as occurring deeper than 75 km. While in practice, the motivation of tsunami prevention disappears for most intermediate and deep sources, the possibility of extending the concept of the mantle magnitude M_m to these events remains an interesting challenge of observational seismology, and is the subject of the present study. Indeed, because of the unfavorable excitation of 20-second surface waves by deep events, M_s is usually not computed for such sources; the only magnitudes remaining in use are body-wave magnitudes, principally m_b (VANĚK *et al.*, 1962). Because m_b is computed at 1 s, it saturates even earlier (around 6.3), and is therefore an even less reliable estimate of the true "size" of the source, correctly described by the seismic moment M_0. Attempts to develop a long-period body-wave magnitude suffer from the limited range of periods contributing to body waves. For example, ABE and KANAMORI'S (1979) m_B is limited in practice to $T \leq 12$ s. Thus, as a variable-period mantle magnitude, M_m clearly has the potential to give a reliable estimate of the seismic moment, while keeping the magnitude concept, i.e., using only one station, and ignoring the exact focal mechanism of the event.

The structure of this paper follows closely that of Paper I. We refer the reader to that previous work, and will emphasize mainly those points characteristic of the deeper nature of the source. We concentrate in the present paper on Rayleigh waves. As discussed in a further section and in a companion paper (OKAL and TALANDIER, 1990; this issue), overtone contamination makes it virtually impossible to extend the concept to Love waves for other than shallow events.

2. *Theory*

As in Paper I, we seek an expression of the mantle magnitude M_m directly related to the seismic moment M_0 through

$$M_m = \log_{10} M_0 - 20 \tag{1}$$

where M_0 is in dyn-cm. Since normal mode excitation theory is applicable for any hypocentral depth, the basic structure of the expression of M_m as a function of spectral amplitude remains

$$M_m = \log_{10} X(\omega) + C_D + C_S - 0.90 \tag{2}$$

where $X(\omega)$ is measured in μm-s.

Source Correction C_S

The frequency-dependent source correction C_S, describing the excitation of Rayleigh waves by a focal source of average geometry, is obviously the parameter which will be most affected by the deeper character of the source. We proceed as in Paper I (see its equations (7)–(9)), and study the variation, both with depth and frequency, of the logarithmic average excitability L_{av}, obtained as the logarithm of the spectral amplitude excited by a unit moment double-couple, averaged over a very large number of source geometries. All computations are made using excitation coefficients derived from normal mode theory, and based on DZIEWONSKI and ANDERSON'S (1981) PREM model.

However, because of the wide range of source depths involved, it is no longer possible to define a correction C_S totally independent of depth. This point is clearly illustrated by the well-known absence of 20 s waves in the record of events around 600 km in depth. Even at periods around 100 s, the excitability of Rayleigh waves decreases by a factor of 25 between 75 and 650 km; if ignored, this situation could lead to magnitude errors as large as ± 0.7 units.

With this in mind, we treat separately earthquakes belonging to three depth windows:

- "Intermediate (A)" events, with depths between 75 and 200 km;
- "Intermediate (B)" events, with depths between 200 and 400 km;
- "Deep" events, with depths greater than 400 km.

This approach has the potential drawback of requiring some estimate of hypocentral depth before a mantle magnitude can be derived. However, our experience in observational seismology suggests that, based on depth phases and the absence of crustal (20 s) Rayleigh waves, the general character (shallow, intermediate, deep) of an earthquake can be assessed quickly during recording, or at the time of the event's location, itself necessary before a magnitude can be computed. In addition, it is fair to recall that all conventional magnitude scales do include some depth dependence, either in the form of an actual correction (e.g., built into the depth-distance term $q(\Delta, h)$ for m_b (VANĚK *et al.*, 1962)), or in the form of a limitation of the applicability of the scale, as would be the case for M_s. We will present in Section 4 some discussion of the effect of misassignment of an earthquake to the wrong depth category.

For each of the depth windows, we then proceed to study the dependence of L_{av} with frequency and true depth. These results are shown in Figures 1, 2 and 3. On each of these figures, the excitability has been plotted as a function of frequency for ten values of the true source depth, identified by symbols 0 (shallowest) to 9 (deepest), in each of the three depth windows considered. These figures are directly comparable to Figure 3 of Paper I. As would be expected from the behavior of the relevant Rayleigh eigenfunctions, the range of scatter of the excitability with true depth increases significantly at the higher frequencies. This leads us to define the following period cut-offs in each of the windows: 90 s for Intermediate (A) events, 140 s for Intermediate (B) events and 190 s for Deep sources.

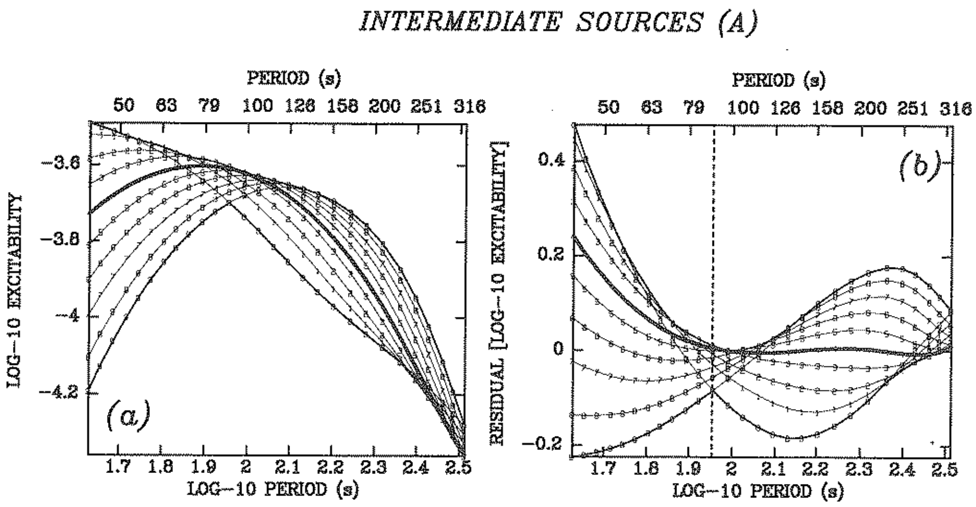

Figure 1

(a): Logarithmic average excitability L_{av}, as defined by Equation (9) of Paper I, plotted as a function of period and depth for Intermediate (A) sources. The symbols (from 0 to 9) refer to 10 sampling depths between 75 and 200 km. The thicker trace corresponds to a depth of 131 km, retained for the computation of C_S. (b): Same as (a), after the correction C_S given by (3a) has been applied. The broken line is the period cutoff (90 s) beyond which the maximum error remains less than ±0.2 orders of magnitude.

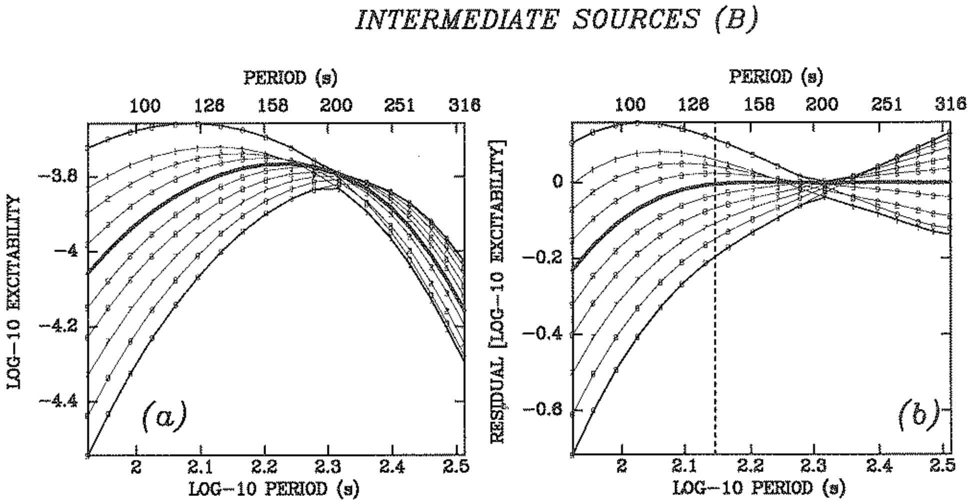

Figure 2

Same as Figure 1, for Intermediate (B) sources. Depths are sampled from 200 to 400 km, and C_S, given by (3b), is computed at 289 km. The cutoff period in (b) is 140 s.

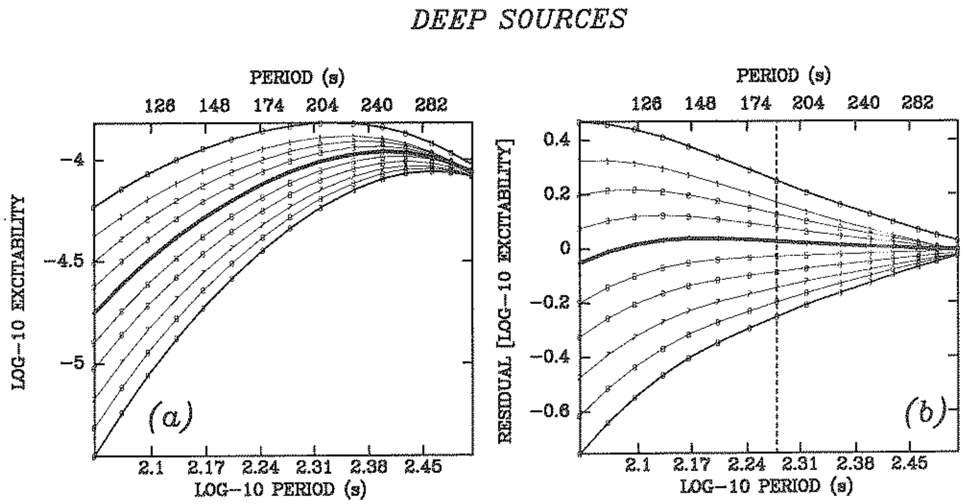

Figure 3
Same as Figure 1, for Deep sources. Depths are sampled from 400 to 670 km, and C_S, given by (3c), is computed at 520 km. The cutoff period in (b) is 190 s.

Following closely the approach in Paper I, and for each of the three depth windows, we use an average value of depth (131, 289 and 529 km, respectively), and model the corresponding values of L_{av} as a function of $\log_{10} T$ using a cubic spline. This yields the following expressions of C_S:

$$C_S = -1.2492\,\theta^3 + 1.9610\,\theta^2 + 1.4812\,\theta + 3.8491 \tag{3a}$$

with $\theta = \log_{10} T - 2.2426$ for Intermediate (A) events ($h = 75$–200 km; $T \geq 90$ s);

$$C_S = 7.2818\,\theta^3 + 5.5164\,\theta^2 + 1.0133\,\theta + 3.8208 \tag{3b}$$

with $\theta = \log_{10} T - 2.3509$ for Intermediate (B) events ($h = 200$–400 km; $T \geq 140$ s); and

$$C_S = 7.6035\,\theta^3 + 7.7495\,\theta^2 - 0.078171\,\theta + 3.9664 \tag{3c}$$

with $\theta = \log_{10} T - 2.4058$ for Deep sources ($h \geq 400$ km; $T \geq 190$ s).

Frames (b) of Figures 1–3 show that the systematic error introduced by replacing L_{av} by its value at the selected hypocentral depth remains less than ± 0.2 unit of magnitude for periods greater than the cut-off periods. On the other hand, if the measurement of M_m is extended to higher frequencies, significant systematic errors could be introduced, which could be as large as 0.7 units, if for example, periods of 80 s were to be used in the case of the deepest earthquakes at the bottom of subduction zones.

We had shown in Paper I that, by scanning a wide range of frequencies for which radiation patterns could take significantly different shapes, and retaining the largest M_m value obtained, our methodology was often successful at avoiding the problems of a station sitting in the node of a radiation pattern. Because the minimum period at which an M_m measurement can be made is significantly increased with respect to the shallow case, we expect to see a decrease in this capacity, in other words to be more prone to underestimation of the size of an event, when dealing with a station located in a node of radiation. This situation cannot be avoided, since it is an expression of the more limited nature of the spectrum excited by a deep earthquake: The absence of significant excitation at higher frequencies can be viewed as a reduction of the dimension of the data space; it should be no surprise that under these conditions, one can retrieve less information on the source. In practice, however, the quality of the results in the present study suggest that this is not an overwhelming problem.

Distance Correction C_D

Since C_D corrects for a path effect independent of the source (see Paper I, Equation (6)), it is obviously independent of source depth, and will keep the same expression as for shallow events. As discussed in Paper I, this distance correction is computed using a regionalized model of Rayleigh wave dispersion and attenuation, or can be further approximated by using the correction C_D^{aver} defined in Section 5 and Table 7 of Paper I. As discussed above, and in order to define a realistic source correction C_S, we had to sharply reduce the frequency range of our measurements. As a result, at the low frequencies involved, the influence of the tectonic structure of the path traveled by the wave is further minimized, and the use of the regionalized model is hardly warranted, especially in the case of "Deep" events. However, for the sake of streamlining our software, we did keep the regionalized corrections in all our intermediate and deep measurements.

3. Application to Data

Our principal goal in this section is to show that realistic estimates of the seismic moment M_0 of intermediate and deep earthquakes can be obtained by computing the value of the mantle magnitude M_m as defined by Equations (2) and (3). Of primary interest will be the comparison of the performance of M_m at various depth levels.

Our dataset for this study consists of 184 GEOSCOPE records for the period 1982–January 1987. In addition, we include 16 records on the ultra-long period "ULP 33" vertical instrument at Pasadena (PAS), including such events as the 1970 Colombia earthquake, at 2×10^{28} dyn-cm the largest deep event ever recorded instrumentally. Figure 4 shows the geographical repartition of sources and stations for each of the three depth windows. While the Intermediate (A), and to a lesser extent the Deep datasets are reasonably dense, the Intermediate (B) dataset suffers from the well-known lower level of seismicity in this depth range: only 8 earthquakes with a maximum moment of just over 1.5×10^{27} dyn-cm could be identified. Figure 5 presents typical examples of the data, and Table 1 lists all relevant hypocentral information, obtained mostly from the "Harvard" centroid moment tensor solutions of DZIEWONSKI *et al.* (1983a–c; 1984a,b; 1985a–c; 1986a,b; 1987a–f; 1988a–c). A variety of other sources are used as references for earlier events.

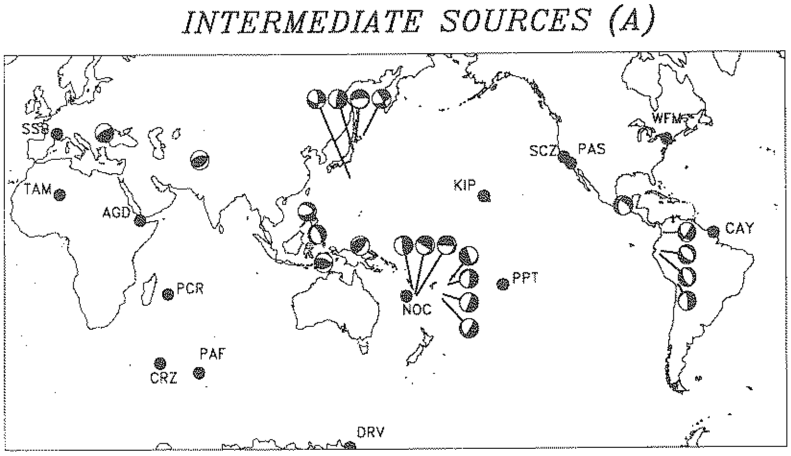

Figure 4a
Map of the earthquake and station distribution for the Intermediate (A) dataset.

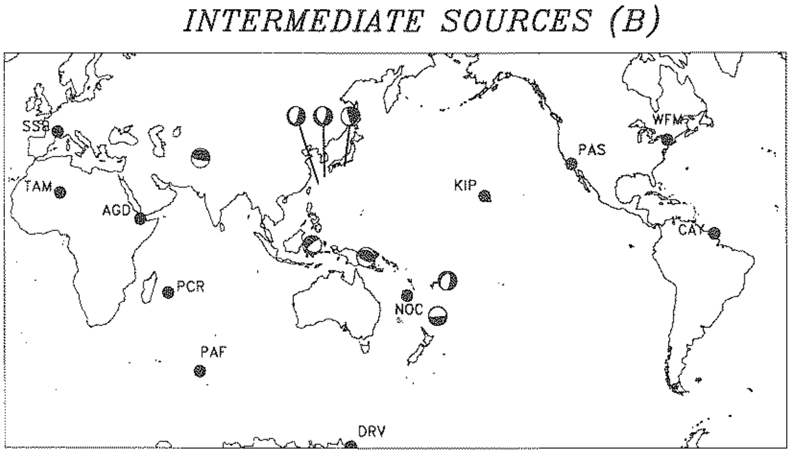

Figure 4b
Map of the earthquake and station distribution for the Intermediate (B) dataset.

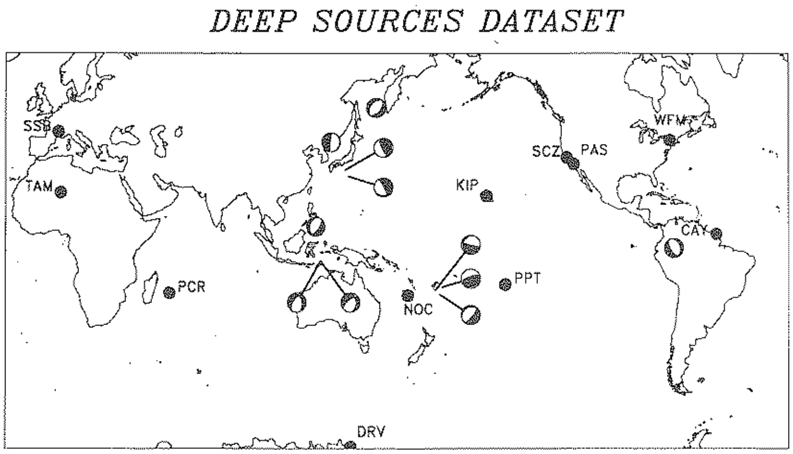

Figure 4c
Map of the earthquake and station distribution for the Deep dataset.

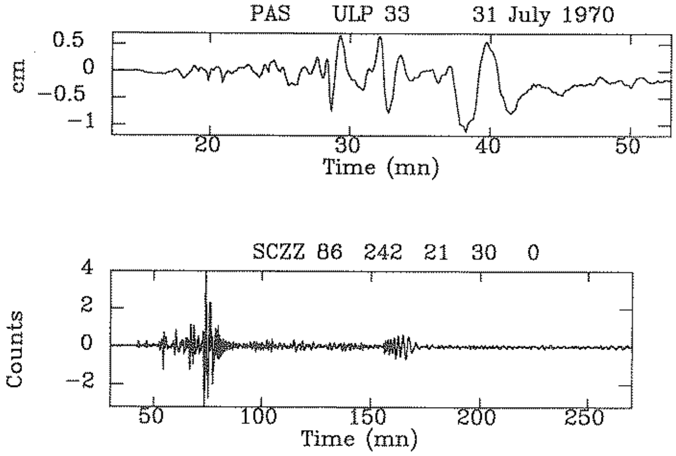

Figure 5
Top: Pasadena ULP-33 record of the 1970 Colombian earthquake. *Bottom:* Typical GEOSCOPE record of an Intermediate (A) earthquake, in this case the 1986 Romanian earthquake, recorded at Santa Cruz, California (SCZ). Note in both cases the presence of overtones preceding the fundamental Rayleigh wave.

It should be noted that one event, on 9 January 1987, lists a depth of only 60 km. This reflects the fact that depths listed in Table 1 are centroid depths resulting from the Harvard inversions, whereas the initial selection of the events was conducted based on PDE depths. This particular event was moved from 98 to 60 km by the Harvard inversion. As will be discussed in more detail later, its inclusion in the dataset does not modify any of our conclusions, and indeed it

Table 1

Source Parameters of Events Used in This Study

	Epicenter		Depth,	Published Moment,	Focal Mechanism			
Date	°N	°E	km	10^{27} dyn-cm	ϕ, deg	δ, deg	λ, deg	Reference
				Intermediate Sources (A)				
1978 12 06	44.59	146.58	181	6.40	64	57	188	a
1979 06 22	17.00	-94.61	117	0.29	190	47	320	b
1979 11 23	4.81	-76.22	109	0.79	137	41	197	b
1980 04 13	-23.47	-177.30	166	2.84	144	25	206	c
1982 06 11	-17.53	-174.46	113	0.20	237	16	322	d
1982 09 06	29.31	140.28	156	0.20	100	55	202	d
1983 02 25	-18.27	-69.44	145	0.13	253	15	346	e
1983 04 12	-4.89	-78.18	111	0.35	339	35	274	f
1983 11 24	-7.55	128.25	157	1.59	74	39	59	g
1984 04 06	-18.93	168.84	175	0.20	304	14	42	h
1984 05 30	-4.88	151.60	157	0.55	246	29	115	h
1984 10 15	-15.74	-173.79	120	0.50	66	15	355	i
1984 11 15	-22.02	170.90	99	0.43	356	27	172	i
1984 11 20	5.21	125.25	181	2.15	172	25	286	i
1985 04 23	15.29	120.60	182	0.21	312	42	319	j
1985 07 29	36.19	70.89	99	1.47	52	38	72	k
1986 01 15	-21.38	170.28	121	0.46	17	28	164	l
1986 08 30	45.55	26.30	133	0.79	39	19	70	m
1986 10 30	-21.69	-176.68	196	0.64	215	5	285	n
1986 11 23	-3.36	-77.47	102	0.19	319	35	278	n
1987 01 09	39.79	141.62	60	0.09	57	13	136	o
1987 01 14	42.56	142.88	89	0.17	52	8	239	o
				Intermediate Sources (B)				
1981 01 02	29.24	128.14	217	0.25	150	34	230	p
1983 01 16	-5.45	147.06	230	0.08	293	30	89	e
1983 01 26	-30.36	-179.43	224	0.37	278	7	282	e
1983 12 30	36.32	70.74	212	1.54	273	18	81	g
1984 01 01	33.40	137.32	384	0.61	31	23	137	q
1984 06 15	-15.79	-174.87	270	0.10	219	31	303	h
1984 08 06	-0.12	122.53	253	1.47	116	33	332	r
1986 05 11	26.68	125.18	204	0.08	169	21	242	s
				Deep Sources				
1970 07 31	-1.46	-72.56	653	20.0	148	58	261	t,u,v
1970 08 30	52.38	151.60	645	1.00	40	50	270	w
1973 09 29	41.90	130.90	575	6.8	186	83	90	u
1978 03 07	31.96	137.61	434	0.54	18	19	133	a
1982 06 22	-7.36	126.12	473	1.77	354	41	220	d
1982 10 07	-7.16	125.91	521	0.13	346	44	230	d
1984 03 05	8.14	123.77	644	0.93	193	34	249	q
1984 03 06	29.36	138.87	446	1.44	68	20	187	q
1984 11 17	-18.74	-178.09	472	0.15	65	19	85	i
1986 05 26	-20.07	178.72	568	0.56	197	21	184	s
1986 06 16	-21.90	-179.04	565	0.45	241	19	290	s

References: a: DZIEWONSKI *et al.* (1987*a*); b: DZIEWONSKI *et al.* (1987*b*); c: DZIEWONSKI *et al.* (1988*a*); d: DZIEWONSKI *et al.* (1983*a*); e: DZIEWONSKI *et al.* (1983*b*); f: DZIEWONSKI *et al.* (1983*c*); g: DZIEWONSKI *et al.* (1984*a*); h: DZIEWONSKI *et al.* (1985*a*); i: DZIEWONSKI *et al.* (1985*b*); j: DZIEWONSKI *et al.* (1986*a*); k: DZIEWONSKI *et al.* (1986*b*); l: DZIEWONSKI *et al.* (1987*c*); m: DZIEWONSKI *et al.* (1987*d*); n: DZIEWONSKI *et al.* (1987*e*); o: DZIEWONSKI *et al.* (1988*a*); p: DZIEWONSKI *et al.* (1988*b*); q: DZIEWONSKI *et al.* (1984*b*); r: DZIEWONSKI *et al.* (1985*c*); s: DZIEWONSKI *et al.* (1987*f*); t: OKAL and GELLER (1979); u: FURUMOTO and FUKAO (1976); v: GILBERT and DZIEWONSKI (1975); w: STRELITZ (1977).

provides an interesting opportunity to test the robustness of our method with respect to errors of assessment of an earthquake depth window.

We limited ourselves mostly to first and second passages of fundamental Rayleigh waves. In Paper I, the motivation of working with higher-order passages was largely to test the adequacy of the dispersion and attenuation models controlling the distance correction C_D. Since this correction is unchanged, this testing is no longer necessary.

An additional problem in selecting the data is the necessity to avoid overtone contamination. For shallow events, the excitation of overtones was in general negligible compared to their fundamental counterparts, but as depth is increased, they become more and more significant contributors to the seismogram (see Figure 5). In general, the most prominent overtone on the vertical component (used exclusively in this study) is the first branch, ${}_1R$, exhibiting prominent periods in the 60–100 s range, and traveling at a group velocity of around 4.4 km/s (OKAL and JO, 1983). Overtone contamination could lead to significant errors since the whole theory underlying the use of M_m is based on the use of a single modal branch. Our procedure in processing the data involved the systematic display of each seismogram, and the visual selection of each time window to be processed.

The computation of M_m proceeds exactly as in the case of shallow events: the time window is Fourier transformed, at each FFT frequency an estimate of M_m is computed, and the maximum value among those retained as the final M_m. For the purpose of assessing the effect of using average values of the hypocentral depth and focal geometry, we also compute the systematic error induced by this procedure, and study the corrected value

$$M_c = M_m + C_{FM} \tag{4}$$

where C_{FM} has the same definition as in Paper I. Similarly, we define the residuals r and r_c as

$$r = M_m - \log_{10} M_0 + 20 \tag{5a}$$

and

$$r_c = M_c - \log_{10} M_0 + 20. \tag{5b}$$

The full dataset, split into the three depth windows, is presented in Table 2, and Table 3 lists the values of the mean residual $\bar{r}$ and of the standard deviation, σ for the whole dataset, as well as for selected sub-datasets. For reference, the corresponding values from Paper I in the case of shallow events, are also listed.

4. *Discussion and Results*

Figure 6 plots the measured values of M_m as a function of the published moments of the events. It is clear that in general the residuals r are comparable to

Table 2

Dataset for Intermediate and Deep Sources

Event	Station	Passage	Δ	M_m^{pub}	M_m	T	r	M_c	r_c
				Intermediate Sources (A)					
1978 12 06	PAS	1	70.22	7.81	8.02	186	0.21	7.88	0.07
1979 06 22	PAS	1	27.17	6.46	6.45	93	-0.01	6.57	0.11
1979 11 23	PAS	1	48.65	6.90	7.29	102	0.39	7.14	0.24
1980 04 13	PAS	1	80.34	7.45	7.20	102	-0.25	7.51	0.06
1982 06 11	PAS	1	74.34	6.30	6.50	114	0.20	6.40	0.10
1982 06 11	SSB	1	152.28	6.30	6.04	256	-0.26	6.55	0.25
1982 06 11	SSB	2	207.72	6.30	6.09	98	-0.21	6.74	0.44
1982 09 06	SSB	1	95.41	6.30	6.65	256	0.35	6.58	0.28
1982 09 06	SSB	2	264.59	6.30	6.60	256	0.30	6.53	0.23
1983 02 25	PAF	1	103.63	6.11	6.03	183	-0.08	6.12	0.01
1983 04 12	PAF	1	119.31	6.54	6.37	98	-0.17	6.59	0.05
1983 04 12	PCR	1	127.75	6.54	6.54	116	0.00	6.68	0.14
1983 04 12	SSB	2	271.66	6.54	6.78	284	0.24	6.67	0.13
1983 04 12	SSB	1	88.34	6.54	6.76	256	0.22	6.80	0.26
1983 11 24	PCR	1	71.18	7.20	7.51	256	0.31	7.43	0.23
1983 11 24	PCR	2	288.82	7.20	7.57	256	0.37	7.49	0.29
1983 11 24	TAM	1	123.02	7.20	7.48	107	0.28	7.61	0.41
1983 11 24	TAM	2	236.98	7.20	7.40	233	0.20	7.46	0.26
1984 04 06	PCR	1	103.41	6.30	6.65	213	0.35	6.28	-0.02
1984 04 06	PCR	2	256.59	6.30	6.78	284	0.48	6.44	0.14
1984 04 06	TAM	1	163.95	6.30	6.69	256	0.39	6.31	0.01
1984 04 06	TAM	2	196.05	6.30	6.56	213	0.26	6.19	-0.11
1984 05 30	PCR	1	93.84	6.74	6.94	183	0.20	6.88	0.14
1984 05 30	SSB	1	130.52	6.74	7.09	116	0.35	6.94	0.20
1984 05 30	SSB	2	229.48	6.74	7.03	197	0.29	6.85	0.11
1984 05 30	TAM	1	142.69	6.74	7.24	91	0.50	7.08	0.34
1984 05 30	TAM	2	217.31	6.74	6.97	160	0.23	6.75	0.01
1984 05 30	WFM	1	124.52	6.74	6.75	213	0.01	6.88	0.14
1984 05 30	WFM	2	235.48	6.74	6.64	233	-0.10	6.78	0.04
1984 10 15	SSB	1	150.47	6.70	6.61	213	-0.09	6.73	0.03
1984 10 15	SSB	2	209.53	6.70	6.59	284	-0.11	6.75	0.05
1984 10 15	WFM	1	107.30	6.70	7.07	256	0.37	6.82	0.12
1984 10 15	WFM	2	252.70	6.70	7.04	256	0.34	6.79	0.09
1984 11 15	SSB	1	154.23	6.63	6.87	183	0.24	6.71	0.08
1984 11 15	SSB	2	205.77	6.63	6.98	213	0.35	6.82	0.19
1984 11 15	PCR	1	103.60	6.63	6.73	256	0.10	6.76	0.13
1984 11 15	PCR	2	256.40	6.63	6.62	183	-0.01	6.70	0.07
1984 11 15	WFM	1	122.50	6.63	6.74	213	0.11	6.73	0.10
1984 11 15	WFM	2	237.50	6.63	6.78	284	0.15	6.72	0.09
1984 11 20	SSB	1	107.13	7.33	7.33	183	0.00	7.41	0.08
1984 11 20	SSB	2	252.87	7.33	7.35	197	0.02	7.41	0.08
1984 11 20	PCR	1	73.14	7.33	7.67	213	0.34	7.35	0.02
1984 11 20	PCR	2	286.86	7.33	7.68	213	0.35	7.36	0.03
1984 11 20	WFM	1	129.03	7.33	7.47	128	0.14	7.37	0.04
1984 11 20	WFM	2	230.97	7.33	7.52	284	0.19	7.35	0.02
1985 04 23	PCR	1	73.43	6.32	6.33	213	0.01	6.40	0.08
1985 04 23	SSB	1	96.46	6.32	7.34	256	1.02	7.10	0.78
1985 04 23	SSB	2	263.54	6.32	7.06	160	0.74	6.89	0.57
1985 04 23	TAM	1	106.00	6.32	6.68	256	0.36	6.47	0.15
1985 04 23	WFM	1	120.60	6.32	6.60	107	0.28	6.53	0.21
1985 04 23	WFM	2	239.40	6.32	6.61	183	0.29	6.47	0.15
1985 07 29	CAY	1	112.97	7.17	7.15	256	-0.02	7.26	0.09
1985 07 29	PCR	1	59.04	7.17	7.21	256	0.04	7.29	0.12
1985 07 29	SSB	1	49.74	7.17	7.26	256	0.09	7.30	0.13
1986 01 15	CAY	1	135.60	6.66	6.42	116	-0.24	6.81	0.15
1986 01 15	NOC	1	3.82	6.66	7.14	256	0.48	7.07	0.41
1986 01 15	PCR	1	103.42	6.66	6.95	256	0.29	6.78	0.12
1986 01 15	SSB	1	153.42	6.66	6.77	213	0.11	6.70	0.04
1986 01 15	TAM	1	165.81	6.66	6.64	107	-0.02	6.83	0.17
1986 01 15	TAM	2	194.19	6.66	6.56	213	-0.10	6.78	0.12
1986 08 30	PAS	1	94.23	6.90	7.29	114	0.39	7.05	0.15

Table 2 (continued)

Dataset for Intermediate and Deep Sources

Event	Station	Passage	Δ	M_m^{pub}	M_m	T	r	M_c	r_c
1986 08 30	PAS	2	265.77	6.90	7.11	186	0.21	6.84	-0.06
1986 08 30	AGD	1	36.77	6.90	7.35	213	0.45	7.09	0.19
1986 08 30	AGD	2	323.23	6.90	7.18	284	0.28	6.95	0.05
1986 08 30	CRZ	1	94.51	6.90	7.42	160	0.52	7.18	0.28
1986 08 30	CRZ	2	265.49	6.90	7.16	256	0.26	6.93	0.03
1986 08 30	DRV	1	140.00	6.90	7.20	107	0.30	6.97	0.07
1986 08 30	DRV	2	220.00	6.90	7.20	233	0.30	6.95	0.05
1986 08 30	KIP	1	113.08	6.90	7.21	98	0.31	7.05	0.15
1986 08 30	KIP	2	246.92	6.90	7.17	284	0.27	7.03	0.13
1986 08 30	PAF	1	102.13	6.90	7.32	183	0.42	7.06	0.16
1986 08 30	PAF	2	257.87	6.90	7.31	284	0.41	7.09	0.19
1986 08 30	PPT	1	151.85	6.90	7.14	213	0.24	6.91	0.01
1986 08 30	PPT	2	208.15	6.90	7.28	284	0.38	7.09	0.19
1986 08 30	RER	1	71.74	6.90	7.31	107	0.41	7.09	0.19
1986 08 30	RER	2	288.26	6.90	7.23	171	0.33	6.97	0.07
1986 08 30	SCZ	2	266.98	6.90	7.26	160	0.36	7.02	0.12
1986 08 30	SCZ	1	93.02	6.90	7.22	213	0.32	6.96	0.06
1986 08 30	SSB	1	15.27	6.90	7.11	107	0.21	7.10	0.20
1986 08 30	TAM	1	28.33	6.90	6.95	183	0.05	7.11	0.21
1986 08 30	TAM	2	331.67	6.90	7.06	284	0.16	7.32	0.42
1986 08 30	TAM	3	388.33	6.90	6.96	197	0.06	7.12	0.22
1986 08 30	WFM	1	67.37	6.90	7.17	98	0.27	6.97	0.07
1986 08 30	WFM	2	292.63	6.90	7.18	213	0.28	6.96	0.06
1986 10 30	PAS	1	78.67	6.81	6.67	146	-0.14	6.68	-0.13
1986 10 30	AGD	1	140.93	6.81	7.25	256	0.44	6.84	0.03
1986 10 30	CRZ	1	99.11	6.81	6.58	284	-0.23	6.81	0.00
1986 10 30	DRV	1	52.64	6.81	6.31	160	-0.50	7.10	0.29
1986 10 30	DRV	1	52.64	6.81	6.31	160	-0.50	7.10	0.29
1986 10 30	KIP	1	46.68	6.81	6.32	98	-0.49	7.09	0.28
1986 10 30	KIP	2	313.32	6.81	6.44	116	-0.37	7.16	0.35
1986 10 30	NOC	1	15.83	6.81	7.24	213	0.43	6.83	0.02
1986 10 30	PAF	1	87.65	6.81	6.87	256	0.06	6.93	0.12
1986 10 30	PPT	1	25.83	6.81	7.27	256	0.46	6.85	0.04
1986 10 30	PPT	2	334.17	6.81	7.24	256	0.43	6.82	0.01
1986 10 30	PPT	3	385.83	6.81	7.29	213	0.48	6.88	0.07
1986 10 30	SSB	1	156.42	6.81	6.90	183	0.09	6.91	0.10
1986 10 30	SSB	2	203.58	6.81	6.92	116	0.11	7.07	0.26
1986 10 30	WFM	1	113.19	6.81	6.99	256	0.18	6.80	-0.01
1986 10 30	WFM	2	246.81	6.81	6.86	116	0.05	6.87	0.06
1986 11 23	AGD	1	120.34	6.28	6.53	256	0.25	6.82	0.54
1986 11 23	CAY	1	26.46	6.28	6.44	256	0.16	6.66	0.38
1986 11 23	CRZ	1	113.24	6.28	6.45	256	0.17	6.80	0.52
1986 11 23	KIP	1	82.45	6.28	6.06	91	-0.22	6.20	-0.08
1986 11 23	SSB	1	86.75	6.28	6.56	256	0.28	6.64	0.36
1986 11 23	TAM	1	84.85	6.28	6.47	256	0.19	6.65	0.37
1986 11 23	WFM	1	45.94	6.28	6.19	91	-0.09	6.15	-0.13
1987 01 09	AGD	1	89.32	5.95	6.13	213	0.18	5.91	-0.04
1987 01 09	CAY	1	133.56	5.95	5.58	91	-0.37	6.01	0.06
1987 01 09	KIP	1	54.06	5.95	6.04	91	0.09	5.78	-0.17
1987 01 09	NOC	1	65.94	5.95	6.13	256	0.18	6.18	0.23
1987 01 09	PPT	1	85.81	5.95	6.00	256	0.05	5.82	-0.13
1987 01 09	SCZ	1	72.25	5.95	5.87	116	-0.08	5.77	-0.18
1987 01 09	SSB	1	86.80	5.95	5.92	256	-0.03	5.92	-0.03
1987 01 14	AGD	1	89.53	6.23	6.21	213	-0.02	6.45	0.22
1987 01 14	AGD	2	270.47	6.23	6.31	233	0.08	6.56	0.33
1987 01 14	CAY	1	130.63	6.23	6.39	183	0.16	6.23	0.00
1987 01 14	CAY	2	229.37	6.23	6.51	256	0.28	6.40	0.17
1987 01 14	CRZ	1	119.83	6.23	6.39	107	0.16	6.44	0.21
1987 01 14	DRV	2	250.92	6.23	6.44	171	0.21	6.24	0.01
1987 01 14	KIP	1	53.23	6.23	5.85	98	-0.38	6.32	0.09
1987 01 14	NOC	1	68.08	6.23	6.56	91	0.33	6.31	0.08
1987 01 14	NOC	2	291.92	6.23	6.72	284	0.49	6.59	0.36

Table 2 (continued)

Dataset for Intermediate and Deep Sources

Event	Station	Passage	Δ	M_m^{pub}	M_m	T	r	M_c	r_c
1987 01 14	PAF	1	111.60	6.23	6.71	116	0.48	6.66	0.43
1987 01 14	PPT	1	86.24	6.23	6.23	256	0.00	6.31	0.08
1987 01 14	PPT	2	273.76	6.23	6.42	197	0.19	6.48	0.25
1987 01 14	SCZ	1	69.97	6.23	6.06	128	-0.17	6.20	-0.03
1987 01 14	SCZ	2	290.03	6.23	6.16	256	-0.07	6.37	0.14
1987 01 14	SSB	1	84.82	6.23	6.48	98	0.25	6.25	0.02
1987 01 14	SSB	2	275.18	6.23	6.47	213	0.24	6.31	0.08
Intermediate Sources (B)									
1981 01 02	PAS	1	91.02	6.40	6.22	146	-0.18	6.20	-0.20
1983 01 16	PAF	1	77.32	5.90	6.23	142	0.33	6.02	0.12
1983 01 16	PCR	1	89.42	5.90	6.16	142	0.26	6.05	0.15
1983 01 16	SSB	1	128.62	5.90	6.28	197	0.38	6.32	0.42
1983 01 26	PAF	1	79.29	6.57	6.80	142	0.23	6.63	0.06
1983 01 26	PAF	2	280.71	6.57	6.80	284	0.23	6.72	0.15
1983 01 26	PCR	1	106.27	6.57	6.78	142	0.21	6.74	0.17
1983 01 26	PCR	2	253.73	6.57	6.69	256	0.12	6.73	0.16
1983 12 30	PAF	1	85.48	7.18	7.47	142	0.29	7.20	0.02
1983 12 30	PAF	2	274.52	7.18	7.53	171	0.35	7.31	0.13
1983 12 30	PCR	1	59.13	7.18	7.59	142	0.41	7.31	0.13
1983 12 30	PCR	2	300.87	7.18	7.45	197	0.27	7.25	0.07
1983 12 30	TAM	1	57.30	7.18	7.15	160	-0.03	7.42	0.24
1983 12 30	TAM	2	302.70	7.18	7.32	142	0.14	7.58	0.40
1984 01 01	PAF	1	101.77	6.79	6.83	256	0.04	6.65	-0.14
1984 01 01	PAF	2	258.23	6.79	6.95	256	0.16	6.77	-0.02
1984 01 01	PCR	1	94.94	6.79	7.04	213	0.25	6.84	0.05
1984 01 01	PCR	2	265.06	6.79	7.10	256	0.31	6.84	0.05
1984 01 01	TAM	1	107.56	6.79	6.79	256	0.00	6.82	0.03
1984 01 01	TAM	2	252.44	6.79	6.85	256	0.06	6.88	0.09
1984 06 15	WFM	1	108.13	6.00	6.13	213	0.13	6.07	0.07
1984 08 06	PCR	1	68.53	7.18	7.14	142	-0.04	7.30	0.12
1984 08 06	PCR	2	291.47	7.18	7.04	183	-0.14	7.22	0.04
1984 08 06	SSB	1	109.42	7.18	7.40	183	0.22	7.23	0.05
1984 08 06	SSB	2	250.58	7.18	7.31	160	0.13	7.12	-0.06
1984 08 06	TAM	1	114.81	7.18	7.36	151	0.18	7.21	0.03
1984 08 06	TAM	2	245.19	7.18	7.22	183	0.04	7.08	-0.10
1986 05 11	AGD	1	78.13	5.90	6.24	142	0.34	5.98	0.08
1986 05 11	CAY	1	148.37	5.90	6.10	197	0.20	6.21	0.31
1986 05 11	KIP	1	69.32	5.90	6.22	151	0.32	6.04	0.14
1986 05 11	NOC	1	62.87	5.90	6.23	183	0.33	6.07	0.17
1986 05 11	SSB	1	90.21	5.90	6.29	142	0.39	6.09	0.19
1986 05 11	TAM	1	103.60	5.90	6.39	142	0.49	6.14	0.24
1986 05 11	WFM	1	108.54	5.90	5.89	142	-0.01	6.15	0.25
Deep Sources									
1970 07 31	PAS	1	55.59	8.30	7.97	219	-0.33	8.22	-0.08
1970 07 31	PAS	2	304.41	8.30	8.05	192	-0.25	8.35	0.05
1970 08 30	PAS	1	63.83	7.00	6.95	205	-0.05	7.13	0.13
1973 09 29	PAS	1	81.24	7.83	7.58	205	-0.25	7.58	-0.25
1978 03 07	PAS	1	82.91	6.73	6.88	205	0.15	6.54	-0.19
1982 06 22	PAS	1	115.39	7.26	6.92	205	-0.34	6.96	-0.30
1982 06 22	PAS	2	244.61	7.26	7.12	205	-0.14	7.16	-0.10
1982 10 07	SSB	1	116.90	6.12	6.38	213	0.26	6.25	0.13
1984 03 05	PCR	1	73.01	6.97	6.96	256	-0.01	7.07	0.10
1984 03 05	SSB	1	103.94	6.97	7.10	256	0.13	7.04	0.07
1984 03 05	TAM	1	112.19	6.97	7.09	256	0.12	7.02	0.05
1984 03 06	SSB	2	265.25	7.16	6.95	197	-0.21	7.86	0.70
1984 03 06	TAM	1	111.31	7.16	6.98	213	-0.18	7.17	0.01
1984 03 06	TAM	2	248.69	7.16	7.10	213	-0.06	7.30	0.14
1984 11 17	SSB	1	153.41	6.16	6.39	213	0.23	6.11	-0.05
1984 11 17	SSB	2	206.59	6.16	6.47	213	0.31	6.19	0.03
1986 05 26	DRV	1	51.70	6.75	6.95	213	0.20	6.81	0.06

Table 2 (continued)

Dataset for Intermediate and Deep Sources

Event	Station	Passage	Δ	M_m^{pub}	M_m	T	r	M_c	r_c
1986 05 26	DRV	2	308.30	6.75	6.93	256	0.18	6.76	0.01
1986 05 26	KIP	1	47.81	6.75	6.86	213	0.11	6.74	-0.01
1986 05 26	KIP	2	312.19	6.75	6.84	256	0.09	6.68	-0.07
1986 05 26	NOC	1	13.63	6.75	6.59	213	-0.16	6.96	0.21
1986 05 26	SSB	1	156.47	6.75	6.92	256	0.17	6.78	0.03
1986 05 26	SSB	2	203.53	6.75	6.93	213	0.18	6.81	0.06
1986 05 26	WFM	1	115.04	6.75	6.82	256	0.07	6.76	0.01
1986 06 16	CAY	1	125.80	6.65	6.84	256	0.19	6.72	0.07
1986 06 16	CAY	2	234.20	6.65	6.82	233	0.17	6.71	0.06
1986 06 16	DRV	1	51.70	6.65	6.64	213	-0.01	6.82	0.17
1986 06 16	DRV	2	308.30	6.65	6.67	256	0.02	6.84	0.19
1986 06 16	KIP	1	47.81	6.65	6.52	256	-0.13	6.76	0.11
1986 06 16	KIP	2	312.19	6.65	6.58	256	-0.07	6.82	0.17
1986 06 16	PPT	1	28.04	6.65	6.84	213	0.19	6.80	0.15
1986 06 16	SCZ	1	79.74	6.65	6.52	256	-0.13	6.83	0.18
1986 06 16	SCZ	2	280.26	6.65	6.54	284	-0.11	6.84	0.19
1986 06 16	SSB	1	156.47	6.65	6.85	256	0.20	6.79	0.14
1986 06 16	SSB	2	203.53	6.65	6.71	233	0.06	6.66	0.01
1986 06 16	WFM	1	115.04	6.65	6.59	256	-0.06	6.83	0.18
1986 06 16	WFM	2	244.96	6.65	6.56	213	-0.09	6.83	0.18

Table 3

Averages and Standard Deviations of the Residuals r

Dataset	Station Code	Number of Records	$\bar{r}$	σ	$\bar{r}_c$	σ_c
Whole dataset		200	0.14	0.23	0.12	0.15
Intermediate (A)		129	0.17	0.24	0.14	0.15
Intermediate (B)		34	0.19	0.16	0.11	0.13
Deep		37	0.01	0.17	0.07	0.16
Shallow Events (from Paper I)		256	0.14	0.25	0.09	0.19
	Individual Stations					
Pasadena (ULP33)	PAS	16	-0.02	0.24	-0.03	0.16
Saint-Sauveur de Badole, France	SSB	38	0.19	0.23	0.17	0.19
Pointe des Cafres, Réunion[†]	PCR, RER	25	0.21	0.17	0.11	0.07
Tamanrasset, Algeria	TAM	23	0.14	0.18	0.16	0.16
Westford, Massachusetts	WFM	20	0.13	0.15	0.09	0.08
Port-aux-Français, Kerguelen Islands	PAF	13	0.21	0.19	0.10	0.13
Kipapa, Hawaii	KIP	12	-0.04	0.27	0.09	0.14
Cayenne, French Guyana	CAY	9	0.06	0.21	0.14	0.12
Papeete, Tahiti	PPT	9	0.27	0.17	0.07	0.11
Dumont d'Urville, Antarctica	DRV	8	0.09	0.25	0.11	0.09
Arga, Djibouti	AGD	8	0.25	0.15	0.17	0.18
Nouméa, New Caledonia	NOC	7	0.30	0.21	0.21	0.13
Santa Cruz, California	SCZ	7	0.02	0.21	0.07	0.12
Crozet Island[††]	CRZ	5	0.18	0.24	0.21	0.19

[†] We treat as a single dataset records from the Réunion Island station before and after it was moved (about 18 km to Rivière de l'Est (RER) in 1986.

[††] Due to the small number of events, the values obtained at Crozet may not be statistically significant.

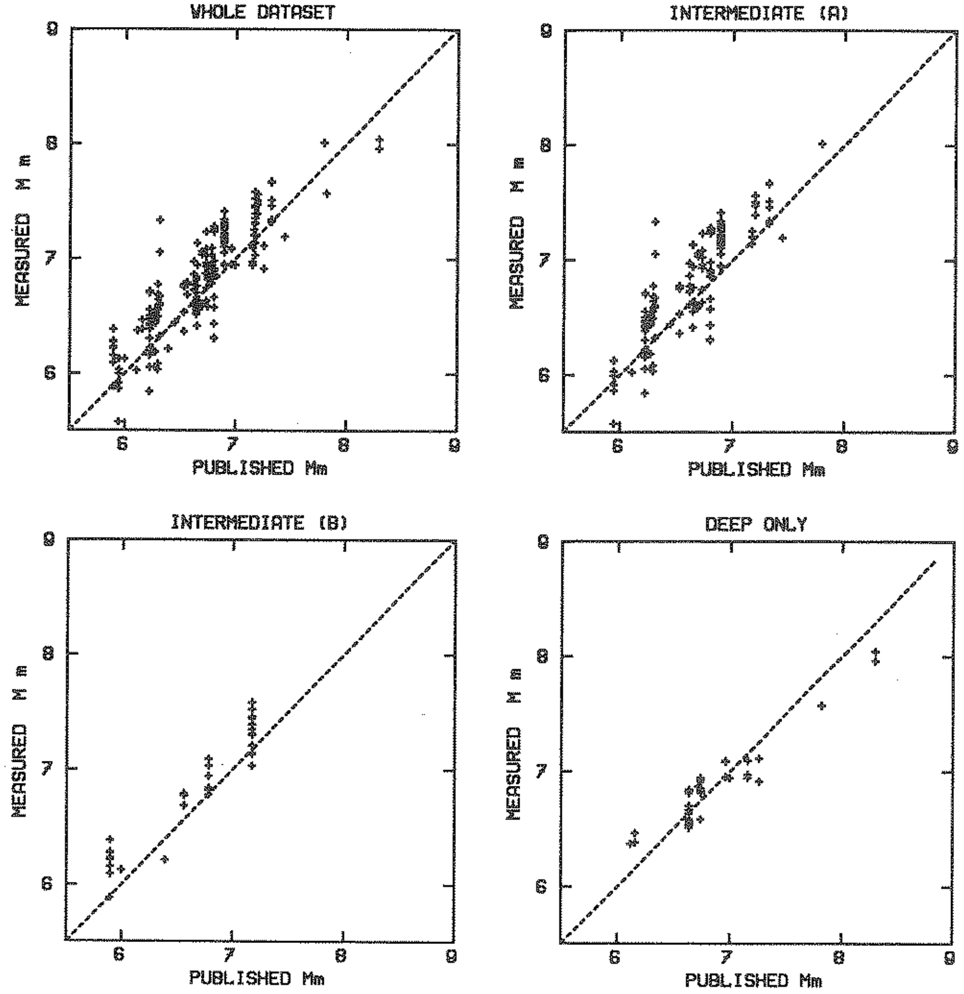

Figure 6
Populations of M_m values plotted as a function of published seismic moment M_0, either as individual datasets for the three depth windows, or a whole dataset (upper left). The dashed lines show the expected relation $M_m = \log_{10} M_0 - 20$.

their counterparts for shallow events studied in Paper I. Coincidentally, the mean residual $\bar{r}$ for both datasets is equal (0.14), and the two standard deviations very comparable (0.23 as opposed to 0.25). Similarly, a large fraction of the individual residuals can be attributed to the influence of ignoring true depth and focal mechanism (σ is reduced nearly in half by considering r_c) but in the present case the average $\bar{r}$ is not reduced significantly. The excellent performance of M_m for the deep sub-dataset $\bar{r} = 0.01$ is probably fortuitous, since its standard deviation remains much larger, and, one focal corrections are applied, $\bar{r}_c$ is actually larger.

A regression of M_m versus the logarithm of published moment yielded a slope of 0.92 for the full dataset, and 1.06 for the large sub-dataset of Intermediate (A) events. These numbers are not significantly different from the value of 1 expected on theoretical grounds. The dataset of Deep events yields a lower slope (0.73), which one could be tempted to interpret as reflecting the initiation of some kind of saturation. However, as shown on Figure 6, this dataset consists of only 14 earthquakes, and the slope is controlled to a large extent by the residuals for the three smallest measurements (positive r), and the two largest ones (negative r). It can be verified that the low value of the slope is actually an artifact of the focal geometries of the three earthquakes involved, and that a slope of 0.92 is obtained if M_c rather then M_m is regressed against $\log_{10}M_0$.

A significant point in this respect is our capability to differentiate between large and truly gigantic deep events, which totally eludes the conventional scale m_b, because of the saturation inherent in the use of higher frequencies. This is best illustrated by comparing the 1970 Colombia earthquake ($M_0 = 2 \times 10^{28}$ dyn-cm) and the 1978 Izu-Bonin shock ($M_0 = 5.4 \times 10^{26}$ dyn-cm), 37 times smaller in published moment. Both events were assigned $m_b = 6.5$ by the ISC, and the USGS/NEIC, probably making use of longer-period body waves, separate them by only 0.2 unit of m_b (7.1 vs. 6.9). On the other hand, M_m values at PAS (8.01 and 6.88) suggest a ratio of about 14 in their seismic moments, despite unfavorable focal geometries.

Finally, the subdataset of Intermediate (B) events, including only 8 earthquakes, is too small to warrant a significant regression of M_m vs $\log_{10}M_0$.

Period

We examine in this section the dependence of the residual populations r and r_c on the period at which the measurement of M_m is made. Figures 7 summarize the results. In general, no significant correlation is found, both for the residuals r and for the values r_c, corrected for true depth and focal mechanism. As more extensively explained in Paper I, this confirms the validity of our Q models, and suggests that our method successfully avoids interference effects stemming from possible source finiteness.

It is interesting to note that the increase in r_c at short periods, identifiable on Figure 13 of Paper I, is absent in the present dataset. This is probably due to the restriction $T \geq 90$ s, strongly curtailing the possibility of multipathing due to lateral heterogeneity.

Possible Station Effects

As in the case of shallower events in Paper I, we also studied the population of residuals at individual stations. These results are included in Table 3, and Figure 8

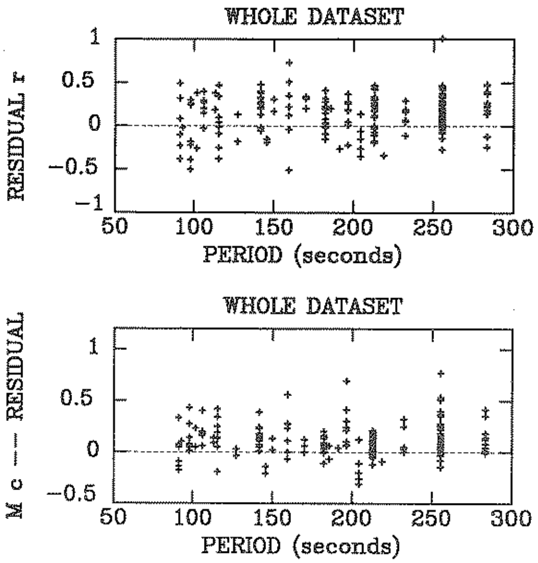

Figure 7

Magnitude residuals plotted as a function of the period T at which the M_m measurement is taken. *Top:* Raw residual r; *Bottom:* Corrected measurements r_c. Note the absence of any trend in these populations.

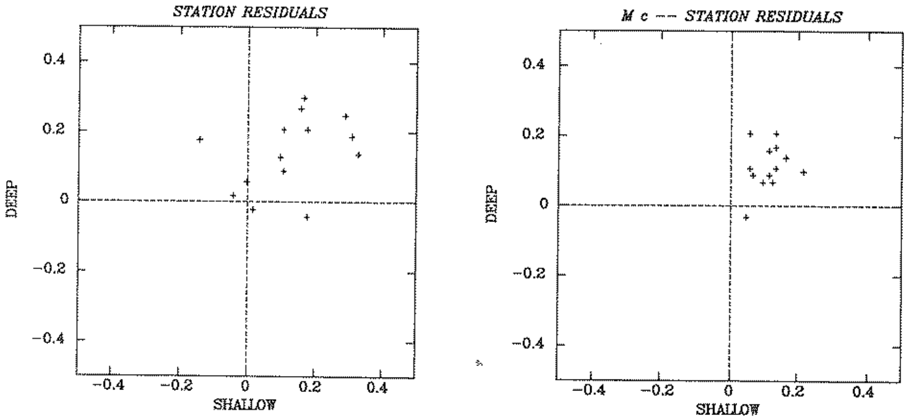

Figure 8

This figure compares the average residuals (in magnitude units) at individual stations, for shallow events (from Paper I), and for the whole intermediate and deep dataset in the present study. Each symbol represents a station. The lack of a systematic trend suggests that no station effects are present. *Left:* Raw residuals $\bar{r}$. *Right:* Corrected residuals $\bar{r}_c$.

looks for a possible correlation between average station residuals for Shallow events on the one hand and Intermediate and Deep ones on the other. The results are largely scattered, and a statistical analysis yields a correlation of only 0.36. A larger correlation coefficient, closer to 1, would indicate some kind of station effect, independent of the depth of the source, and suggest the possible definition of station corrections, analogous to those often used with higher-frequency magnitude scales. As already concluded in Paper I, most of the scatter between station residuals is an artifact of the geometry of focal mechanism and station-epicenter geometries. Indeed, the correlation coefficient falls to 0.26 if the residuals $\bar{r}_c$ are used.

Possible Systematic Errors in Depth Assignment

In this section, we explore the possible systematic errors in our estimate of the seismic moment which could stem from assigning the earthquake to the wrong depth window. We are motivated in this respect by the example mentioned earlier of the earthquake on 09 January 1987, for which we used a PDE depth of 98 km, but a centroid depth of 60 km was computed by the Harvard inversion. As a first step, we study as a function of frequency the difference between the two source correction terms $C_S^{\mathrm{Int(A)}}$ and C_S^{Shallow}. Results, plotted on Figure 9, can be interpreted in the following way: Assume a Shallow event featuring a "perfect" source spectrum (M_m constant with frequency) is mistakenly interpreted as Intermediate (A). The computation uses $C_S^{\mathrm{Int(A)}}$ instead of C_S^{Shallow}, and as a result, selects to compute M_m at the longer periods, overestimating it by about 0.2 units. However, this pertains to a "perfect" source, which would have to be located at the 20 km depth selected for modeling C_S^{Shallow}. In reality, it is far more likely that an event mistakenly taken as Intermediate (A) would be towards the deep end of the shallow

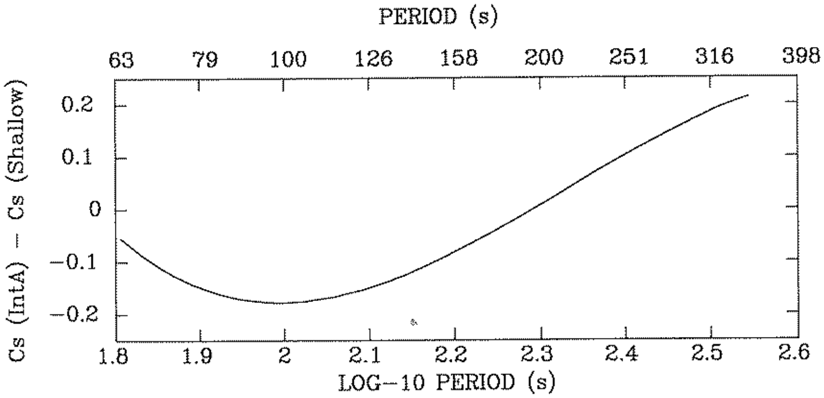

Figure 9

Difference $C_S^{\mathrm{Int(A)}} - C_S^{\mathrm{Shallow}}$ of the station corrections relative to the two classes of events, plotted as a function of period. This curve is representative of the error which may be involved when an earthquake is misassigned to the wrong depth window. See text for details.

group, i.e., around 60–75 km in depth. In this case, the lines labeled 8 and 9 on Figure 3b of Paper I, illustrate that the excitability at such depths is underestimated (by about 0.1 unit) around 60 s, and overestimated (by about 0.1 unit) at very long periods, by the standard 20-km spline. These lines actually show the variation of M_m, computed for this event and with a shallow correction, as a function of frequency. They indicate that the program will select the value around 60 s, overestimating the moment of the event by about 0.1 unit of magnitude. Now, if this 60–75 km deep earthquake is inadvertently modeled as Intermediate (A), the error involved can be obtained by adding the curve on Figure 9, and the lines 8 or 9 on Figure 3b of Paper I. The two curves compensate each other to some extent, and the result should stay within ± 0.1 unit of magnitude, with M_m computed using $C_S^{\mathrm{Int(A)}}$ expected to slightly overestimate the true size of the event, by retaining a value at a longer period.

In the converse case of an Intermediate (A) event (roughly 100 km in true depth), inadvertently treated as Shallow, a similar discussion would show that the program will elect to compute a shorter period M_m (roughly 60 s), again overestimating the true earthquake size by 0.1 to 0.2 units of magnitude.

Regarding the 9 January 1987 event South of Japan, we have further explored this situation by treating the earthquake both as Intermediate (A) (values reported in Table 2), and Shallow (these values are given in Table 4). Contrary to our expectations, the latter are in general slightly greater than the former. This is due to the very special nature of the focal mechanism of the event (approaching pure dip-slip on a vertical fault), an effect not included in the above discussion. An interesting case is Station CAY, located in a strong node of radiation for most mantle periods: because of the more stringent limitation on the range of frequencies, the intermediate depth algorithm fails to retrieve significant energy from the seismogram and underestimates the moment significantly, whereas the shallow one manages to find substantial amplitude at the shorter-period end of the spectrum (64 s).

Table 4

M_m Values Computed for the 09 January, 1987 Event, Interpreted as Either Shallow or Intermediate (A)

Station	Δ	Published	Computed M_m					
	(°)	M_m	Intermediate (A)			Shallow		
			M_m	Period	r	M_m	Period	r
AGD	89.32	5.95	6.13	213	0.18	6.25	64	0.30
CAY	133.56	5.95	5.58	91	-0.37	6.12	64	0.17
KIP	54.06	5.95	6.04	91	0.09	6.31	67	0.36
NOC	65.94	5.95	6.13	256	0.18	6.18	71	0.23
PPT	85.81	5.95	6.00	256	0.05	6.25	71	0.30
SCZ	72.25	5.95	5.87	116	-0.08	6.03	107	0.08
SSB	86.80	5.95	5.92	256	-0.03	6.12	85	0.17

In concluding this section, both theoretical and experimental studies suggest that misassignment of an event to the wrong depth window should not result in errors greater than 0.2 units of magnitude, except possibly in unfavorable focal geometry and station azimuth combinations. The latter disclaimer should not be surprising, since it is fundamentally inherent in the approach we have taken in the development of the magnitude M_m.

5. Conclusion

We have presented an extension of the mantle magnitude M_m proposed for shallow events by OKAL and TALANDIER (1989), to intermediate and deep earthquakes. Our method allows the real-time estimate of their seismic moment, with an average accuracy of 0.15 units of magnitude, and a standard deviation of ± 0.23 units, corresponding to an uncertainty of a multiplicative or divisive factor of 1.69 on the value of the seismic moment. These numbers are fully comparable to their counterparts for shallow events.

While the tsunami warning motivation disappears at the greater depths, the example of the 1970 Colombia earthquake demonstrates the power of our method in allowing immediate recognition of truly gigantic, very deep shocks. At such depths, because of the absence of 20-second surface waves, the body-wave m_b, saturating around 6.3, is the only traditional magnitude reported. Conversely, we have shown that M_m gives a reasonable estimate of the size of such events, properly described by their seismic moment M_0, while keeping the basic philosophy of the magnitude approach: a real-time measurement, made on a single station, and ignoring the geometrical details of the source.

In addition, we believe that the method can be successfully applied to the study of the seismic moment of historical deep shocks, for which there often exist only a very limited supply of records, preventing in most cases the compilation of a satisfactory focal solution.

Acknowledgements

The original development of the mantle magnitude M_m was a joint venture with Jacques Talandier, and its extension to deeper sources obviously owes much to him. I am grateful to Barbara Romanowicz for providing a regular flow of GEOSCOPE data, and to my colleagues at Caltech for access to the PAS archives. John Woodhouse provided computerized datasets of centroid moment tensor solutions in advance of publication. This research was supported by the National Science Foundation under Grant Number EAR-87-20549.

REFERENCES

ABE, K., and KANAMORI, H. (1979), *Temporal Variation of the Activity of Intermediate and Deep Focus Earthquakes*, J. Geophys. Res. *84*, 3589–3595.

DZIEWONSKI, A. M., and ANDERSON, D. L. (1981), *Preliminary Reference Earth Model*, Phys. Earth Planet. Inter. *25*, 297–356.

DZIEWONSKI, A. M., FRIEDMAN, A., GIARDINI, D., and WOODHOUSE. J. H. (1983a), *Global Seismicity of 1982: Centroid Moment Tensor Solutions for 308 Earthquakes*, Phys. Earth Planet. Inter. *33*, 76–90.

DZIEWONSKI, A. M., FRIEDMAN, A., and WOODHOUSE, J. H. (1983b), *Centroid Moment-tensor Solutions for January–March 1983*, Phys. Earth Planet. Inter. *33*, 71–75.

DZIEWONSKI, A. M., FRANZEN, J. E., and WOODHOUSE, J. H. (1983c), *Centroid Moment-tensor Solutions for April–June 1983*, Phys. Earth Planet. Inter. *33*, 243–249.

DZIEWONSKI, A. M., FRANZEN, J. E., and WOODHOUSE, J. H. (1984a), *Centroid Moment-tensor Solutions for October–December 1983*, Phys. Earth Planet. Inter. *34*, 129–136.

DZIEWONSKI, A. M., FRANZEN, J. E., and WOODHOUSE, J. H. (1984b), *Centroid Moment-tensor Solutions for January–March 1984*, Phys. Earth Planet. Inter. *34*, 209–219.

DZIEWONSKI, A. M., FRANZEN, J. E., and WOODHOUSE, J. H. (1985a), *Centroid Moment-tensor Solutions for April–June 1984*, Phys. Earth Planet. Inter. *37*, 87–96.

DZIEWONSKI, A. M., FRANZEN, J. E., and WOODHOUSE, J. H. (1985b), *Centroid Moment-tensor Solutions for October–December 1984*, Phys. Earth Planet. Inter. *39*, 147–156.

DZIEWONSKI, A. M., FRANZEN, J. E., and WOODHOUSE, J. H. (1985c), *Centroid Moment-tensor Solutions for July–September 1984*, Phys. Earth Planet. Inter. *38*, 203–213.

DZIEWONSKI, A. M., FRANZEN, J. E., and WOODHOUSE, J. H. (1986a), *Centroid Moment-tensor Solutions for April–June 1985*, Phys. Earth Planet. Inter. *41*, 215–224.

DZIEWONSKI, A. M., FRANZEN, J. E. and WOODHOUSE, J. H. (1986b), *Centroid Moment-tensor Solutions for July–September 1985*, Phys. Earth Planet. Inter. *42*, 205–214.

DZIEWONSKI, A. M., EKSTRÖM, G., FRANZEN, J. E., and WOODHOUSE, J. H. (1987a), *Global Seismicity of 1978; Centroid Moment-tensor Solutions for 512 Earthquakes*, Phys. Earth Planet. Inter. *46*, 316–342.

DZIEWONSKI, A. M., EKSTRÖM, G., FRANZEN, J. E., and WOODHOUSE, J. H. (1987b), *Global Seismicity of 1979; Centroid Moment-tensor Solutions for 524 Earthquakes*, Phys. Earth Planet. Inter. *48*, 18–46.

DZIEWONSKI, A. M., FRANZEN, J. E., and WOODHOUSE, J. H. (1987c), *Centroid Moment-tensor Solutions for January–March 1986*, Phys. Earth Planet. Inter. *45*, 1–10.

DZIEWONSKI, A. M., EKSTRÖM, G., FRANZEN, J. E., and WOODHOUSE, J. H. (1987d), *Centroid Moment-tensor Solutions for July–September 1986*, Phys. Earth Planet. Inter. *46*, 305–315.

DZIEWONSKI, A. M., EKSTRÖM, G., WOODHOUSE, J. H., and ZWART, G. (1987e), *Centroid Moment-tensor Solutions for October–December 1986*, Phys. Earth Planet. Inter. *48*, 5–17.

DZIEWONSKI, A. M., EKSTRÖM, G., FRANZEN, J. E., and WOODHOUSE, J. H. (1987f), *Centroid Moment-tensor Solutions for April–June 1986*, Phys. Earth Planet. Inter. *45*, 229–239.

DZIEWONSKI, A. M., EKSTRÖM, G., FRANZEN, J. E., and WOODHOUSE J. H. (1988a), *Global Seismicity of 1980; Centroid Moment-tensor Solutions for 515 Earthquakes*, Phys. Earth Planet. Inter. *50*, 127–154.

DZIEWONSKI, A. M., EKSTRÖM, G., WOODHOUSE, J. H., and ZWART, G. (1988b), *Centroid Moment-tensor Solutions for January–March 1987*, Phys. Earth Planet. Inter. *50*, 116–126.

DZIEWONSKI, A. M., EKSTRÖM, G., FRANZEN, J. E., and WOODHOUSE, J. H. (1988c), *Global Seismicity of 1981; Centroid Moment-tensor Solutions for 542 Earthquakes*, Phys. Earth Planet. Inter. *50*, 155–182.

FURUMOTO, M., and FUKAO, Y. (1976), *Seismic Moments of Great Deep Shocks*, Phys. Earth Planet. Inter. *11*, 352–357.

GILBERT, J. F., and DZIEWONSKI, A. M. (1975), *An Application of Normal Mode Theory to the Retrieval of Structural Parameters and Source Mechanism from Seismic Spectra*, Phil. Trans. Roy. Soc. London *278A*, 187–269.

OKAL, E. A. (1979), *Higher Mode Rayleigh Waves Studied as an Individual Seismic Phase*, Earth Plan. Sci. Lett. *43*, 162–167.

OKAL, E. A., and GELLER, R. J. (1979), *On the Observability of Isotropic Seismic Sources: The July 31, 1970 Colombian Earthquake*, Phys. Earth Planet Inter. *18*, 176–196.

OKAL, E. A., and JO, B.-G. (1983), *Regional Dispersion of First-order Overtone Rayleigh Waves*, Geophys. J. Roy. Astr. Soc. *72*, 461–481.

OKAL, E. A., and TALANDIER, J. (1989), *M_m: A Variable Period Mantle Magnitude*, J. Geophys. Res. *94*, 4169–4193.

OKAL, E. A., and TALANDIER, J. (1990), *M_m: Extension to Love Waves of the Concept of a Variable-period Mantle Magnitude*, Pure Appl. Geophys. *134*, 355–384.

STRELITZ, R. A., *Source Processes of Three Complex Deep-focus Earthquakes*, Ph.D. Dissertation, (Princeton University, Princeton, N.J. 1977), 259 pp.

TALANDIER, J., and OKAL, E. A. (1989), *An Algorithm for Automated Tsunami Warning in French Polynesia, Based on Mantle Magnitudes*, Bull. Seismol. Soc. Am. *79*, 1177–1193.

VANĚK, J., ZÁTOPEK, A., KÁRNÍK, V., KONDORSKAYA, N. V., RIZNICHENKO, YU. V., SAVARENSKII, E. F., SOLOV'EV, S. L., and SHEBALIN, N. V. (1962), *Standardization of Magnitude Scales*, Izv. Akad. Nauk SSSR, Ser. Geofiz. *2*, 153–158.

(Received August 10, 1989, accepted May 1, 1990)